ACSNANO
www.acsnano.org
ARTICLE

Atomic Scale Imaging of Nucleation and Growth Trajectories of an Interfacial Bismuth Nanodroplet

Yingxuan Li,*[,†] Benjamin R. Bunes,[‡] Ling Zang,[‡] Jie Zhao,[†] Yan Li,[†] Yunqing Zhu,[†] and Chuanyi Wang*[,†]

[†]Laboratory of Environmental Sciences and Technology, Xinjiang Technical Institute of Physics & Chemistry, Key Laboratory of Functional Materials and Devices for Special Environments, Chinese Academy of Sciences, Urumqi, 830011, China

[‡]Nano Institute of Utah and Department of Materials Science and Engineering, University of Utah, Salt Lake City, Utah 84112, United States

Supporting Information

ABSTRACT: **Because of the lack of experimental evidence, much confusion still exists on the nucleation and growth dynamics of a nanostructure, particularly of metal. The situation is even worse for nanodroplets because it is more difficult to induce the formation of a nanodroplet while imaging the dynamic process with atomic resolution. Here, taking advantage of an electron beam to induce the growth of Bi nanodroplets on a $SrBi_2Ta_2O_9$ platelet under a high resolution transmission electron microscope (HRTEM), we directly observed the detailed growth pathways of Bi nanodroplets from the earliest stage of nucleation that were previously inaccessible. Atomic scale imaging reveals that the dynamics of nucleation involves a much more complex trajectory than previously predicted based on classical nucleation theory (CNT). The monatomic Bi layer was first formed in the nucleation process, which induced the formation of the prenucleated clusters. Following that, critical nuclei for the nanodroplets formed both directly from the addition of atoms to the prenucleated clusters by the classical growth process and indirectly through transformation of an intermediate liquid film based on the Stranski−Krastanov growth mode, in which the liquid film was induced by the self-assembly of the prenucleated clusters. Finally, the growth of the Bi nanodroplets advanced through the classical pathway and sudden droplet coalescence. This study allows us to visualize the critical steps in the nucleation process of an interfacial nanodroplet, which suggests a revision of the perspective of CNT.**

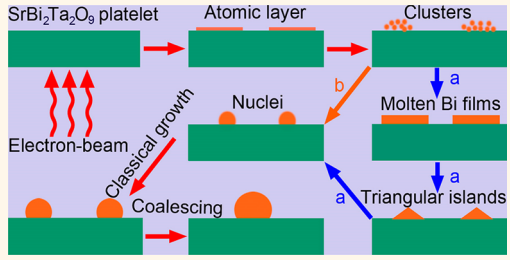

KEYWORDS: *in situ imaging, atomic resolution, Bi nanodroplet, nucleation, growth*

The study of the growth mechanisms of nanostructures is a critical topic in chemistry and materials science because it may provide necessary insights to guide the creation of new materials with novel and interesting properties. Generally, the growth phenomena involve the birth and subsequent growth of critical nuclei. In the two processes, the nucleation stage may play a decisive role in determining the properties of the new phases such as the growth rate and transition mechanism, which are the central problems of emerging new phases.[1] Classical nucleation theory (CNT) has widely been used to describe the nucleation process, which was first studied by Gibbs for the nucleation of water droplets from condensation of vapor (Scheme 1).[2−4] According to the CNT, the nucleation of a new phase is energetically favorable only when its nucleus reaches a critical size. Recently, it was demonstrated that intermediate phases exist before the formation of the nucleus. For example, it was recently reported that $CaCO_3$ nucleation occurs from prenucleated stable clusters, which is not predicted by CNT.[5,6] Furthermore, it

Scheme 1. Schematic Illustration of the Classical Model for Droplet Nucleation

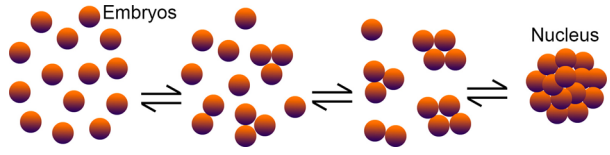

was proven that many nucleation processes do not proceed via the classical pathway. For instance, a two-step nucleation, leading to a significant enhancement of nucleation rates for crystallization in solution, has been demonstrated in many systems. On the basis of this theory, the denser liquid precursors,[7−11] amorphous precursors,[12] or clusters of mole-

Received: November 15, 2015
Accepted: January 11, 2016
Published: January 11, 2016

DOI: 10.1021/acsnano.5b07197
ACS Nano 2016, 10, 2386−2391

cules[13,14] can serve as a metastable intermediate in a nucleation process.

Compared to the nucleation of solid phases, much less is known about the behavior of interfacial nanodroplets from the early nucleation stage to the liquid dynamics, although scientific interests in droplets are ever increasing from both fundamental science[15,16] and applications.[17−19] It has been assumed that droplet nucleation is based on simple CNT since the study on the nucleation of water droplets by Gibbs more than 130 years ago.[2−4] Recently, the Stranski−Krastanov growth model was proven suitable for describing the transition from layers to micrometer-sized droplets.[20] However, no direct observations of the growth dynamics of a nanodroplet have been performed to explore how the structure evolves from the earliest nucleation stage. It is well-known that the microscopic process of actual nucleation is always much more complex, and little is known about the prenucleation stage (the very early stage of the nucleation).[5] Therefore, detecting the intermediate metastable states in a nucleation pathway is essential for understanding the fundamental mechanisms that give birth to droplet nuclei. Furthermore, the nanoscale dynamics of an interfacial liquid, which might diverge significantly from the behavior of bulk ones, is a highly debated topic, and most of what is known is from computational simulations.[21] Therefore, it is necessary to develop an experimental technique in which the formation of a nanodroplet and the imaging of the dynamic process from nucleation can be simultaneously achieved.

Recently, *in situ* imaging or measurement based on atomic force microscopy (AFM),[22] scanning tunneling microscopy (STM),[23] X-ray absorption fine structure (XAFS) spectroscopy,[24,25] and (scanning) transmission electron microscopy ((S)TEM)[26−28] have been developed to address the technical challenge in observing nanostructure growth. Among these approaches, *in situ* TEM has a unique advantage of directly observing both the structural and morphological changes of nanoparticles with temporal and spatial resolution.[29] This was first demonstrated in the pioneering work of Williams et al., in which they developed a liquid cell reactor to image the dynamic growth of Cu clusters on a surface by using a TEM with a resolution of 5 nm.[26] In addition, Alivisatos and co-workers observed the growth trajectories of colloidal platinum nanoparticles initiated by 2.2 nm particles, indicating that the nanoparticle coalescence acts as a driving force in nanocrystal growth.[30] More recently, Zheng et al. observed the shape evolution of Pt−Fe nanorods by *in situ* TEM in solution.[31] Unfortunately, those studies used relatively thick Si_3N_4 or SiO_2 windows which have poor electron transmittance and result in a resolution limit of only a few nanometers. Most recently, to overcome that challenge, Alivisatos and his co-workers used a liquid cell reactor with graphene windows to study Pt nanoparticle growth with atomic resolution.[32] Although the *in situ* observation provides dynamic information on growth mechanisms of nanocrystals such as nanoparticles, and nanorods, *etc.*, the nucleation and growth pathways of liquid nanodroplets are largely unexplored, mainly because of the experimental difficulties in manipulating growth of the nanodroplets and monitoring the growth process simultaneously. Although the dynamics of nanodroplet nucleation and growth on self-supported thin films has been studied,[33] direct observation of the details of the nucleation process at atomic scale in real time and space is still lacking.

In an earlier work, we studied the *in situ* growth of bismuth (Bi) nanoparticles on the surface of $SrBi_2Ta_2O_9$ (SBT) platelets under ultraviolet (UV) light illumination in aqueous glucose solutions.[34] Bismuth is an important material across many fields including catalysis,[35] thermoelectricity,[36] and superconductivity,[37] and fabricating supported nanoparticles is a significant step toward fabricating devices. However, our previous results show that nanoparticle growth is very slow under UV light irradiation. Beyond light irradiation, recent works established the ability to fabricate nanostructures under electron-beam irradiation.[38−41] In this work, Bi nanodroplet growth on SBT was simultaneously induced and imaged from the earliest stage of nucleation under electron-beam irradiation in a HRTEM. The *in situ* HRTEM observation provides detailed information on the initial stage of nucleation that is usually too small for a direct experimental determination of their structure and formation mechanism. Furthermore, the subsequent growth dynamics of the nanodroplets was also studied in real space and time. This experimental system enables us to explore the complex dynamics during the formation of Bi nanodroplets with atomic resolution, which is valuable for understanding the heterogeneous nucleation and growth process in general.

RESULTS AND DISCUSSION

A $SrBi_2Ta_2O_9$ (SBT) platelet was prepared by a molten salt route as reported in our previous work and used as substrate for Bi nanoparticle growth.[34] Figure 1a shows a typical HAADF-STEM image of a 15 nm nanoparticle grown on a SBT platelet after 20 min of electron-beam irradiation. To confirm the composition of the nanoparticle, energy dispersive spectroscopy (EDS) analysis was performed on an individual nanoparticle anchored to the edge of the platelet (Figure 1b). The EDS result clearly reveals that the nanoparticle is composed of elemental Bi. Besides Bi, C and Cu are also observed, which originate from the carbon-coated copper grid used in HRTEM observation for supporting the sample. Therefore, it is confirmed that pure metallic Bi was formed on the SBT platelet by electron-beam irradiation.

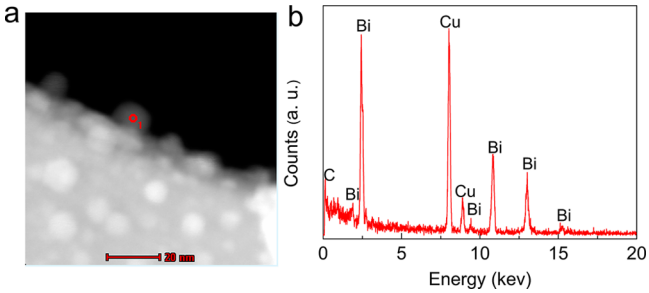

Figure 1. (a) The image obtained by high-angle annular dark-field scanning transmission electron microscopy (HAADF-STEM). (b) EDS analysis of a single Bi nanoparticle anchored to the edge of $SrBi_2Ta_2O_9$ platelet, as marked by the red circled region in (a).

In order to investigate the growth trajectories of the Bi nanostructures clearly, we focused our study on nanostructures anchored to the edge of the SBT platelet. The growth of Bi nanostructures was recorded *in situ* as videos (Videos S1−S3). Figure 2 shows a series of snapshots from the HRTEM video (Video S1) of the edge of an SBT platelet recorded at different exposure durations of electron-beam irradiation. It is observed that after 48 s of electron-beam irradiation, a nanostructure forms on the edge of the SBT platelet in the shape of a spherical cap, with the contact angle θ_0 (Figure 2j). Under the

DOI: 10.1021/acsnano.5b07197
ACS Nano 2016, 10, 2386−2391

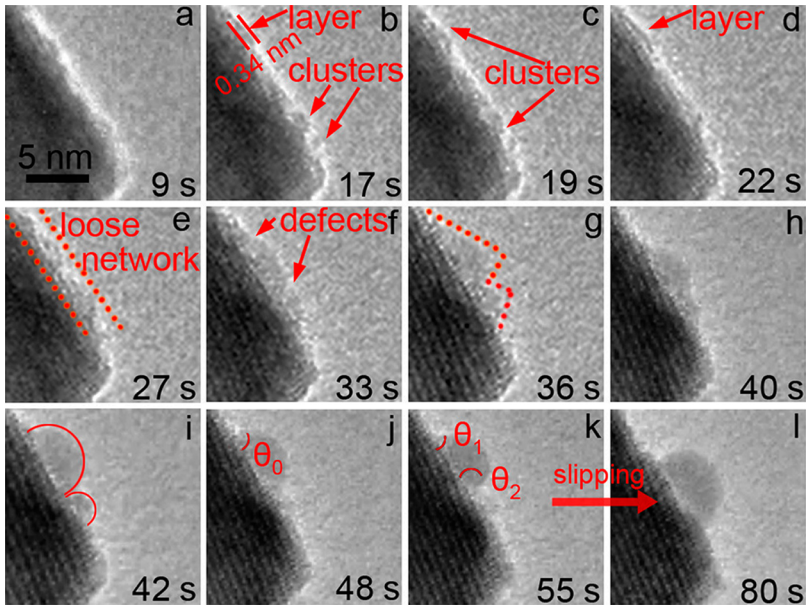

Figure 2. Sequential snapshots from *in situ* HRTEM showing different stages of the growth process of an individual nanodroplet through transformation of the liquid Bi film.

same 200 keV electron-beam irradiation, advancing and receding of contact angles were observed (Figure 2k), while the nanostructure was mobile on the surface of the SBT substrate (see Video S1 for details). The deviation of both contact angles from the static contact angle is characteristic of droplets and is known as contact-angle hysteresis.[21] Furthermore, a slip process of the nanostructure was also observed between 55 and 80 s. This motion is also a characteristic of liquid droplets, where the redistribution of atoms in the nanodroplet overcomes interfacial forces of the substrate.[21] Therefore, it is suggested that the particle observed is molten under electron-beam irradiation. The incident electron irradiation can create a significant temperature rise in the material due to electron thermal spikes and poor thermal conduction away from the particles.[42] Considering the low melting point of bulk Bi (271.5 °C) and the further decrease in this equilibrium temperature with the decrease in particle size,[43] it is reasonable to assume that the 200 keV electron beam can maintain the Bi nanodroplets in a liquid phase.

Further analysis of the HRTEM video allowed, for the first time, the study of the growth mechanism of the liquid nanodroplet from the initial stage of nucleation. As seen in Video S1, the intermediate states are formed within the few seconds needed to focus and adjust the electron-beam. When clear images were first taken, a thin film had already formed on one lateral side of the platelet as shown in Video S1. Fortunately, no noticeable Bi morphologies such as films or islands (Figure 2a) formed on the other side of the platelet, making it suitable for a complete investigation of the Bi nanodroplet formation from the initial stage of nucleation under electron-beam irradiation.

Figures 2b–i show a magnified view of a single nucleation event (see more details in Video S1). Initially, the Bi (III) in SBT was reduced to Bi atoms by electron-beam irradiation. At 17 s, a film with a thickness of around 0.34 nm is layered atop the SBT substrate (Figure 2b), confirming that the film is a monatomic Bi layer because the Bi–Bi distance in bulk bismuth is around 0.3 nm.[44] As shown in Figures 2b–d, a metastable state with fluctuation between Bi clusters and the monatomic Bi layer was observed between 17 and 22 s. This fluctuation may result from the collective effect of the SBT–Bi and the Bi–Bi interactions. As more and more Bi atoms were reduced and migrated to the substrate surface, we can directly observe from Video S1 (between 22 and 27 s) that the Bi atoms in the monatomic layer interact with the adjacent atoms (or the atoms subsequently formed in SBT) to form bigger Bi clusters, which aggregate into a loose network (Figure 2e). In this process, the clusters frequently changed their positions, sizes (both increasing and decreasing), and shape as shown in Video S1, indicating that the freshly formed clusters are highly active on the substrate. The competition between entropy and attractive interactions between the Bi atoms might be the driving force for the formation of the clusters.[45]

Under electron-beam irradiation, the addition of Bi atoms and densification of the aggregated clusters lead to the formation of a liquid film with two defect sites (as marked by red arrows in Figure 2f). As irradiation continues, the two defects serve as nucleation centers for the formation of an uneven structure composed of two triangular-shaped islands (Figure 2g) at the expense of the Bi film, which further develop into two spherical caps connected with a bridge at 40 s (Figure 2h). As an intermediate state, the triangular-shaped islands are kinetically controlled, resulting from the anisotropic diffusion of the Bi atoms in the growing clusters. Moreover, the shape evolution of the Bi clusters from triangular to circular might be affected by surface tension. Uniform contrast of the spherical cap indicates the liquid nature of the clusters, confirming the formation of the critical nucleus for the nanodroplet. It can be concluded from Figure 2 that the unique nucleation process of the nanodroplet follows a path from monatomic layer to atomic clusters to the flat film to triangular-shaped islands and ultimately to the critical nucleus, which can be used as a guideline for future investigations of the nucleation process of the nanodroplet. As shown in Video S1, the bigger droplet grows by Bi addition from SBT and the Laplace pressure-induced flow from the smaller one (Figures 2h,i).[46] Ultimately, a single droplet is formed as shown in Figure 2j and Video S1. On the basis of the above observation, we can conclude that the

DOI: 10.1021/acsnano.5b07197
ACS Nano 2016, 10, 2386–2391

formation of a 3D nanodroplet from a flat 2D film could be explained by the Stranski–Krastanov mode,[20] which has been used to fabricate semiconductor nanoparticles by the self-assembly of 2D films.[47] Although evidence of Stranski–Krastanov growth of the droplets was provided by AFM imaging,[20] to the best of our knowledge, this is the first time a group has directly observed the details in nucleation stage for a metal nanodroplet with atomic resolution.

The formation process of the other nanodroplet is shown in Figure 3. The nanodroplet under investigation is the lowermost

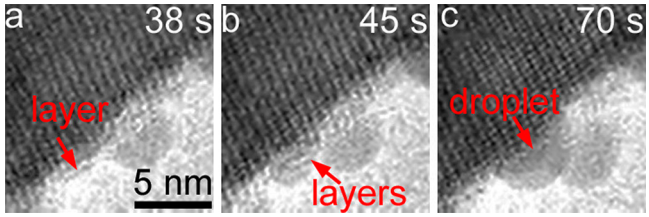

Figure 3. Sequential snapshots from *in situ* HRTEM showing different stages of the growth process of an individual nanodroplet from aggregation of the clusters.

one shown in the Video S1. As shown in Figure 3a, a monatomic Bi layer was also formed initially, which was similar to that observed in Figure 2. Under continuous irradiation, a spherical cluster with a layered structure forms by the self-assembly of the preformed clusters (Figure 3b). To the best of our knowledge, the formation of the layering structure on the nucleation pathway of a droplet has not been observed previously in experimental or theoretical studies. As shown in Figure 3c, based on the layering structure, a critical nucleus with a size of about 5 nm forms by the addition of atoms (see more details in Video S1). On the basis of the above observations, it can be concluded that multiple nucleation pathways for Bi nanodroplets simultaneously exist: directly from the aggregation of the Bi clusters (Figure 3) and indirectly through the transformation of the liquid Bi film (Figure 2).

As shown in Video S1, the nanodroplet in Figure 2j exhibits continuous growth. The growth dynamics of the nanodroplet viewed by HRTEM between 64 and 82 s is shown in Figure 4a and c. At this time, the lattice spacing of the SBT could be clearly detected, as shown in Figure 4a. Figure 4b shows the temporal dependence of the size of the nanodroplet between 64 and 82 s corresponding to Figures 4a and c. The size was measured from the area of semicircular nanodroplet shape in the HRTEM image. It can be seen from Figure 4b that the nanodroplet size increases with the irradiation time. However, the growth velocity of the nanodroplet rapidly decreases with increasing size of the nanodroplet. The HRTEM method also allowed us to study the growth trajectory of an individual nanodroplet in atomic resolution, as shown in Video S1 and Figure 4c. Very small black spots exhibiting a diameter of a single atom (about 0.3 nm), which could be reduced Bi atoms, appear gradually from the SBT bulk and then land on the surface of SBT (Figure 4c). The Bi atoms exist for extremely short times (<1 s) after which they are adsorbed by the nanodroplet (see details in Video S1). On the interface, more than 10 events of atom landing on the nanodroplet from the edge of the SBT were observed. This phenomenon suggests that the classical growth process that predicts monomer attachment to the growing nanostructures can play a role in nanodroplet growth. Although the classical growth process is well accepted in the field, the *in situ* observation of this process with atomic resolution in real time and space is still difficult to achieve. This detailed view may provide information for understanding the growth behavior of supported nanostructures.

In addition to the observed classical growth, the real-time HRTEM investigation also shows that further growth of the nanodroplets is dominated by droplet coalescence events (see Videos S2 and S3). Videos S2 and S3 were recorded after 160 and 394 s electron-beam illumination, respectively. Single frames from Videos S2 and S3 show the top (Figure 5a) and

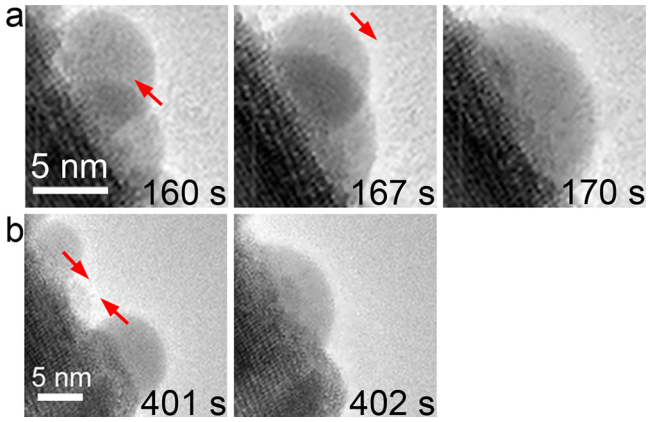

Figure 5. Sequential snapshots from the *in situ* HRTEM video shows the top (a) and side (b) views of the coalescence events of the nanodroplets.

side (Figure 5b) views of two different coalescence events of the Bi nanodroplets. From Figure 5a, it can be seen that the droplet below moves at 167 s with an increase in overlapped portion and then is covered by the upper one immediately to complete the coalescence process. Another coalescence process is shown in Video S3. It can be seen clearly from Video S3 that

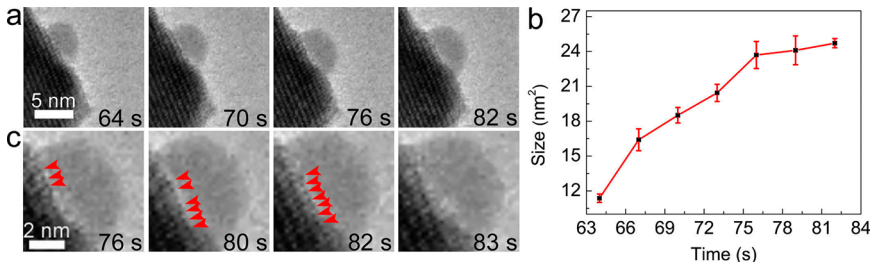

Figure 4. (a) *In situ* HRTEM images of nanodroplet growth between 64 and 82 s. (b) Growth dynamics of the nanodroplet as a function of time. (c) Magnified images of the nanodroplet in Video S1 showing the classical growth model of the nanodroplet.

DOI: 10.1021/acsnano.5b07197
ACS Nano 2016, 10, 2386–2391

two liquid droplets collide with a fast velocity. After two droplets collide head-on, they form a bigger droplet. The driving force for the coalescence process is caused by surface energy reduction resulting from the reduced total surface area of both droplets. Moreover, our observation shows an interesting phenomenon that the coalescence of Bi nanodroplets is abrupt at a critical point, which was predicted for the coalescence of metal clusters by theoretical simulation.[48] As we know, the dynamics of droplet coalescence relates with many physical, chemical, and biological phenomena and is of great potential for a variety of important applications, which makes the phenomenon interesting for experimental and theoretical studies.[21]

The present study provides not only a promising approach to fabricate nanodroplets at nanometer range (<5 nm) but also a method to achieve *in situ* HRTEM observation on the growth dynamics of nanodroplets. On the basis of the above observations, the evolution pathway of Bi nanodroplets can be summarized in Scheme 2. Two alternative routes for the growth of Bi nanodroplets are involved: one proceeds as route "a" in Scheme 2, *i.e.*, monolayer → cluster → liquid film → critical nucleus → nanodroplet; and the other follows route "b" in Scheme 2, *i.e.*, monolayer → cluster → critical nucleus → nanodroplet. Both the cluster and liquid film can coexist as the intermediate state during nucleation, suggesting the complexity of the growth process of interfacial Bi nanodroplet formation.

Scheme 2. Schematic Illustration of Overall Growth Trajectories of the Interfacial Bi Nanodroplet under Electron-Beam Irradiation in HRTEM

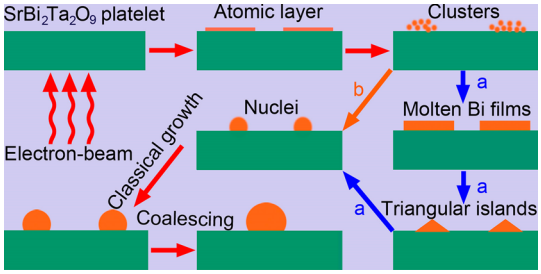

CONCLUSIONS

In conclusion, we have demonstrated a new approach to observe the *in situ* formation of Bi nanodroplets from SBT under electron-beam irradiation in HRTEM. Atomic scale imaging shows, for the first time, the microscopic details of the process that distinguish the different stages before nucleation. Evolution of Bi nanodroplets consists mainly of three stages: (i) generating atomic Bi layers followed by the formation of an atomic cluster or liquid film; (ii) forming critical nuclei for the nanodroplets both directly from the addition of atoms via the classical pathway and indirectly through transformation of the liquid Bi film based on the Stranski–Krastanov growth mode; and finally, (iii) growth of nanodroplets through the addition of atoms and droplet coalescence. These observations provide a unique view on the formation pathway of individual nanodroplets on substrates, which will contribute greatly to our understanding of the growth mechanisms of nanodroplets from the earliest stage of nucleation. Moreover, our findings will be helpful in advancing the general understanding of nucleation in nanoscale systems.

METHODS

Sample Preparation. $SrBi_2Ta_2O_9$ was prepared by a molten salt method published before.[34] In a typical synthesis, nitrate ($Sr(NO_3)_2$, 99%) and oxides (Bi_2O_3 and Ta_2O_5, 99.9%) in appropriate stoichiometric amounts according to the composition of $SrBi_2Ta_2O_9$ were mixed with NaCl and KCl (1:1 molar ratio), followed by grinding for 30 min. The synthesis precursor and the two chlorides were mixed at a 1:1 weight ratio; the chlorides were used as solvent when melted. The reaction mixture was then loaded into an alumina crucible and heated at 850 °C for 3 h, followed by cooling to room temperature in air. The resulting product was washed thoroughly with deionized water to remove the chlorides and then dried at 50 °C for 3 h.

HRTEM Observation and EDS Analysis. The formation of Bi nanocrystals was initiated by electron-beam irradiation on a $SrBi_2Ta_2O_9$ platelet housed in the same TEM (JEOL model JEM-2100), which was also used for the atomic structural imaging of the Bi nanoparticles. The TEM was operated at an accelerating voltage of 200 keV. Images and videos were recorded using a CCD camera (Gatan 832). EDS was performed on a FEI Tecnai F30 electron microscope after the $SrBi_2Ta_2O_9$ sample was irradiated by an electron beam for 20 min.

ASSOCIATED CONTENT

Supporting Information

Videos S1 to S3 and their captions. The Supporting Information is available free of charge on the ACS Publications website at DOI: 10.1021/acsnano.5b07197.

Description and captions of the videos (PDF)
Real-time HRTEM imaging of motion of a Bi nanodroplet induced by electron-beam irradiation (AVI)
Details of the coalescence between Bi nanodroplets under electron-beam irradiation (AVI)
Details of the coalescence between Bi nanodroplets under electron-beam irradiation (AVI)

AUTHOR INFORMATION

Corresponding Authors

*(Y.L.) E-mail: yxli@ms.xjb.ac.cn.
*(C.W.) E-mail: cywang@ms.xjb.ac.cn.

Notes

The authors declare no competing financial interest.

ACKNOWLEDGMENTS

This work was supported by the National Natural Science Foundation of China (Grant Nos. U1403193 and 21173261), the "Western Light" Program of Chinese Academy of Sciences (Grant No.YB201303), the Excellent Youth Foundation of Xinjiang Uygur Autonomous Region (Grant No. 2013711004), and the CAS/SAFEA International Partnership Program for Creative Research Teams.

REFERENCES

(1) Erdemir, D.; Lee, A. Y.; Myerson, A. S. Nucleation of Crystals from Solution: Classical and Two-Step Models. *Acc. Chem. Res.* **2009**, *42*, 621–629.
(2) Gibbs, J. W. On the Equilibrium of Heterogeneous Substances. *Trans. Conn. Acad. Arts Sci.* **1876**, *3*, 108–248.
(3) Gibbs, J. W. On the Equilibrium of Heterogeneous Substances. *Trans. Conn. Acad. Arts Sci.* **1878**, *16*, 343–524.
(4) Sleutel, M.; Van Driessche, A. E. S. Role of Clusters in Nonclassical Nucleation and Growth of Protein Crystals. *Proc. Natl. Acad. Sci. U. S. A.* **2014**, *111*, E546–E553.
(5) Gebauer, D.; Volkel, A.; Cölfen, H. Stable Prenucleation Calcium Carbonate Clusters. *Science* **2008**, *322*, 1819–1822.

DOI: 10.1021/acsnano.5b07197
ACS Nano 2016, 10, 2386–2391

(6) Pouget, E. M.; Bomans, P. H. H.; Goos, J. A. C. M.; Frederik, P. M.; De With, G.; Sommerdijk, N. A. J. M. The Initial Stages of Template-Controlled $CaCO_3$ Formation Revealed by Cryo-TEM. *Science* **2009**, *323*, 1455−1458.
(7) Ten Wolde, P. R.; Frenkel, D. Enhancement of Protein Crystal Nucleation by Critical Density Fluctuations. *Science* **1997**, *277*, 1975−1978.
(8) Kimura, M. Characterization of the Dense Liquid Precursor in Homogeneous Crystal Nucleation Using Solution State Nuclear Magnetic Resonance Spectroscopy. *Cryst. Growth Des.* **2006**, *6*, 854−860.
(9) Stradner, A.; Sedgwick, H.; Cardinaux, F.; Poon, W. C. K.; Egelhaaf, S. U.; Schurtenberger, P. Equilibrium Cluster Formation in Concentrated Protein Solutions and Colloids. *Nature* **2004**, *432*, 492−495.
(10) Savage, J. R.; Dinsmore, A. D. Experimental Evidence for Two-Step Nucleation in Colloidal Crystallization. *Phys. Rev. Lett.* **2009**, *102*, 198302.
(11) Vekilov, P. G. Nucleation. *Cryst. Growth Des.* **2010**, *10*, 5007−5019.
(12) Nielsen, M. H.; Aloni, S.; De Yoreo, J. J. *In Situ* TEM Imaging of $CaCO_3$ Nucleation Reveals Coexistence of Direct and Indirect Pathways. *Science* **2014**, *345*, 1158−1162.
(13) Garetz, B. A.; Matic, J.; Myerson, A. S. Polarization Switching of Crystal Structure in the Nonphotochemical Light-Induced Nucleation of Supersaturated Aqueous Glycine. *Phys. Rev. Lett.* **2002**, *89*, 175501.
(14) Yau, S.-T.; Vekilov, P. G. Quasi-Planar Nucleus Structure in Apoferritin Crystallization. *Nature* **2000**, *406*, 494−497.
(15) Podgorski, T.; Flesselles, J.-M.; Limat, L. Corners, Cusps, and Pearls in Running Drops. *Phys. Rev. Lett.* **2001**, *87*, 036102.
(16) Varagnolo, S.; Ferraro, D.; Fantinel, P.; Pierno, M.; Mistura, G.; Amati, G.; Biferale, L.; Sbragaglia, M. Stick-Slip Sliding of Water Drops on Chemically Heterogeneous Surfaces. *Phys. Rev. Lett.* **2013**, *111*, 066101.
(17) Yao, X.; Hu, Y.; Grinthal, A.; Wong, T.; Mahadevan, L.; Aizenberg, J. Adaptive Fluid-Infused Porous Films with Tunable Transparency and Wettability. *Nat. Mater.* **2013**, *12*, 529−534.
(18) Gau, H.; Herminghaus, S.; Lenz, P.; Lipowsky, R. Liquid Morphologies on Structured Surfaces: From Microchannels to Microchips. *Science* **1999**, *283*, 46−49.
(19) Ledesma-Aguilar, R.; Nistal, R.; Hernández-Machado, A.; Pagonabarraga, I. Controlled Drop Emission by Wetting Properties in Driven Liquid Filaments. *Nat. Mater.* **2011**, *10*, 367−371.
(20) Song, J.; Li, Q.; Wang, X.; Li, J.; Zhang, S.; Kjems, J.; Besenbacher, F.; Dong, M. Evidence of Stranski−Krastanov Growth at the Initial Stage of Atmospheric Water Condensation. *Nat. Commun.* **2014**, *5*, 4837.
(21) Mirsaidov, U. M.; Zheng, H.; Bhattacharya, D.; Casana, Y.; Matsudaira, P. Direct Observation of Stick-Slip Movements of Water Nanodroplets Induced by an Electron Beam. *Proc. Natl. Acad. Sci. U. S. A.* **2012**, *109*, 7187−7190.
(22) Yau, S.-T.; Vekilov, P. G. Direct Observation of Nucleus Structure and Nucleation Pathways in Apoferritin Crystallization. *J. Am. Chem. Soc.* **2001**, *123*, 1080−1089.
(23) Stabel, A.; Heinz, R.; De Schryver, F. C.; Rabe, J. P. Ostwald Ripening of Two-Dimensional Crystals at the Solid-Liquid Interface. *J. Phys. Chem.* **1995**, *99*, 505−507.
(24) Yao, T.; Sun, Z.; Li, Y.; Pan, Z.; Wei, H.; Xie, Y.; Nomura, M.; Niwa, Y.; Yan, W.; Wu, Z.; Jiang, Y.; Liu, Q.; Wei, S. Insights into Initial Kinetic Nucleation of Gold Nanocrystals. *J. Am. Chem. Soc.* **2010**, *132*, 7696−7701.
(25) Yao, T.; Liu, S.; Sun, Z.; Li, Y.; He, S.; Cheng, H.; Xie, Y.; Liu, Q.; Jiang, Y.; Wu, Z.; Pan, Z.; Yan, W.; Wei, S. Probing Nucleation Pathways for Morphological Manipulation of Platinum Nanocrystals. *J. Am. Chem. Soc.* **2012**, *134*, 9410−9416.
(26) Williamson, M. J.; Tromp, R. M.; Vereecken, P. M.; Hull, R.; Ross, F. M. Dynamic Microscopy of Nanoscale Cluster Growth at the Solid-liquid Interface. *Nat. Mater.* **2003**, *2*, 532−536.
(27) Chai, J.; Liao, X.; Giam, L. R.; Mirkin, C. A. Nanoreactors for Studying Single Nanoparticle Coarsening. *J. Am. Chem. Soc.* **2012**, *134*, 158−161.
(28) Kimura, Y.; Niinomi, H.; Tsukamoto, K.; García-Ruiz, J. M. *In Situ* Live Observation of Nucleation and Dissolution of Sodium. *J. Am. Chem. Soc.* **2014**, *136*, 1762−1765.
(29) Liao, H.-G.; Niu, K.; Zheng, H. Observation of Growth of Metal Nanoparticles. *Chem. Commun.* **2013**, *49*, 11720−11727.
(30) Zheng, H. M.; Smith, R. K.; Jun, Y. W.; Kisielowski, C.; Dahmen, U.; Alivisatos, A. P. Observation of Single Colloidal Platinum Nanocrystal Growth Trajectories. *Science* **2009**, *324*, 1309−1312.
(31) Liao, H.-G.; Cui, L.; Whitelam, S.; Zheng, H. Real-Time Imaging of Pt_3Fe Nanorod Growth in Solution. *Science* **2012**, *336*, 1011−1014.
(32) Yuk, J. M.; Park, J.; Ercius, P.; Kim, K.; Hellebusch, D. J.; Crommie, M. F.; Lee, J. Y.; Zettl, A.; Alivisatos, A. P. High-Resolution EM of Colloidal Nanocrystal Growth Using Graphene Liquid Cells. *Science* **2012**, *336*, 61−64.
(33) Barkay, Z. Dynamic Study of Nanodroplet Nucleation and Growth on Self-Supported Nanothick Liquid Films. *Langmuir* **2010**, *26*, 18581−18584.
(34) Li, Y.; Zang, L.; Li, Y.; Liu, Y.; Liu, C.; Zhang, Y.; He, H.; Wang, C. Photoinduced Topotactic Growth of Bismuth Nanoparticles from Bulk $SrBi_2Ta_2O_9$. *Chem. Mater.* **2013**, *25*, 2045−2051.
(35) Yu, H.; Li, J.; Loomis, R. A.; Gibbons, O. C.; Wang, L.-W.; Buhro, W. E. Cadmium Selenide Quantum Wires and the Transition from 3D to 2D Confinement. *J. Am. Chem. Soc.* **2003**, *125*, 16168−16169.
(36) Heremans, J. P.; Thrush, C. M.; Morelli, D. T.; Wu, M.-C. Thermoelectric Power of Bismuth Nanocomposites. *Phys. Rev. Lett.* **2002**, *88*, 216801.
(37) Tian, M.; Wang, J.; Kumar, N.; Han, T.; Kobayashi, Y.; Liu, Y.; Mallouk, T. E.; Chan, M. H. W. Observation of Superconductivity in Granular Bi Nanowires Fabricated by Electrodeposition. *Nano Lett.* **2006**, *6*, 2773−2780.
(38) Wahl, R.; Mertig, M.; Raff, J.; Selenska-Pobell, S.; Pompe, W. Electron-Beam Induced Formation of Highly Ordered Palladium and Platinum Nanoparticle Arrays on the S Layer of Bacillus Sphaericus NCTC 9602. *Adv. Mater.* **2001**, *13*, 736−740.
(39) Motte, L.; Urban, J. Silver Clusters on Silver Sulfide Nanocrystals: Synthesis and Behavior after Electron Beam Irradiation. *J. Phys. Chem. B* **2005**, *109*, 21499−21501.
(40) Zhu, J.; Sun, T.; Hng, H. H.; Ma, J.; Boey, F. Y. C.; Lou, X.; Zhang, H.; Xue, C.; Chen, H.; Yan, Q. Fabrication of Core−Shell Structure of M@C (M = Se, Au, Ag_2Se) and Transformation to Yolk−Shell Structure by Electron Beam Irradiation or Vacuum Annealing. *Chem. Mater.* **2009**, *21*, 3848−3852.
(41) Yao, L.; Majumdar, S.; Äkäslompolo, L.; Inkinen, S.; Qin, Q. H.; Dijken, S. Electron−Beam−Induced Perovskite−Brownmillerite−Perovskite Structural Phase Transitions in Epitaxial $La_{2/3}Sr_{1/3}MnO_3$ Films. *Adv. Mater.* **2014**, *26*, 2789−2793.
(42) Yokota, T.; Murayama, M.; Howe, J. M. *In situ* Transmission-Electron-Microscopy Investigation of Melting in Submicron Al-Si Alloy Particles under Electron-Beam Irradiation. *Phys. Rev. Lett.* **2003**, *91*, 265504.
(43) Goswami, R.; Chattopadhyay, K. Melting of Bi Nanoparticles Embedded in a Zn Matrix. *Acta Mater.* **2004**, *52*, 5503−5510.
(44) Chen, J.; Wu, L.-M.; Chen, L. Syntheses and Characterizations of Bismuth Nanofilms and Nanorhombuses by the Structure-Controlling Solventless Method. *Inorg. Chem.* **2007**, *46*, 586−591.
(45) Laaksonen, A. A Unifying Model for Adsorption and Nucleation of Vapors on Solid Surfaces. *J. Phys. Chem. A* **2015**, *119*, 3736−3745.
(46) Sharma, A.; Khanna, R. Pattern Formation in Unstable Thin Liquid Films. *Phys. Rev. Lett.* **1998**, *81*, 3463.
(47) Yang, B. Elastic Energy Release Rate of Quantum Islands in Stranski−Krastanow Growth. *J. Appl. Phys.* **2002**, *92*, 3704−3710.
(48) Yu, X.; Duxbury, P. M. Kinetics of Nonequilibrium Shape Change in Gold Clusters. *Phys. Rev. B: Condens. Matter Mater. Phys.* **1995**, *52*, 2102.

DOI: 10.1021/acsnano.5b07197
ACS Nano 2016, 10, 2386−2391